DOI: 10.1002/ejic.200900677

Dinuclear Oxidovanadium(IV) and Dioxidovanadium(V) Complexes of 5,5′-Methylenebis(dibasic tridentate) Ligands: Synthesis, Spectral Characterisation, Reactivity, and Catalytic and Antiamoebic Activities

Mannar R. Maurya,*[a] Aftab Alam Khan,[a] Amir Azam,[b] Amit Kumar,[c] Samir Ranjan,[d] Neelima Mondal,[d] and J. Costa Pessoa*[c]

Keywords: Vanadium / EPR spectroscopy / NMR spectroscopy / Catalytic activity / Antiamoebic activity

The synthesis of dinuclear oxidovanadium(IV) and dioxidovanadium(V) complexes of two hydrazones [$CH_2(H_2$sal-nah)$_2$ (**I**) and $CH_2(H_2$sal-inh)$_2$ (**II**)] derived from 5,5′-methylenebis(salicylaldehyde) [CH_2(Hsal)$_2$] and nicotinic acid hydrazide (nah) or isonicotinic acid hydrazide (inh) is described. The compounds were characterised in the solid state and in solution, namely by spectroscopic techniques (IR, UV/Vis, EPR, ^{1}H, ^{13}C and ^{51}V NMR). It has been demonstrated that the dioxidovanadium(V) complexes $K_2[CH_2\{V^VO_2$(sal-nah)$\}_2]\cdot 2H_2O$ (**3**), $Cs_2[CH_2\{V^VO_2$(sal-nah)$\}_2]\cdot 2H_2O$ (**4**) and $Cs_2[CH_2\{V^VO_2$(sal-inh)$\}_2]\cdot 2H_2O$ (**5**) of **I** and **II** are active in the oxidative bromination of salicylaldehyde by H_2O_2, therefore acting as functional models of vanadium-dependent haloperoxidases, and it has also been shown that the corresponding oxidovanadium(IV) complexes [$CH_2\{V^{IV}O$(sal-nah)$(H_2O)\}_2$] (**1**) and [$CH_2\{V^{IV}O$(sal-inh)$(H_2O)\}_2$] (**2**) are catalyst precursors for the catalytic oxidation, by peroxide, of methyl phenyl sulfide and diphenyl sulfide, yielding the corresponding sulfoxide and sulfone. Plausible intermediates involved in these catalytic processes are established by UV/Vis, EPR and ^{51}V NMR studies. The dioxidovanadium(V) complexes along with ligands **I** and **II** were also screened against HM1:1MSS strains of *Entamoeba histolytica*. The results showed that the IC_{50} values of compounds **3** and **5** are lower than the IC_{50} value of metronidazole. The toxicity studies against human cervical (HeLa) cell lines showed that compounds **3** and **5** are not much toxic but are more toxic than metronidazole.

Introduction

The discovery of vanadium-dependent haloperoxidase enzymes and the catalytic potential of several model vanadium complexes in oxidation and oxygen-transfer reactions, including the oxidative halogenation of organic substrates[1–5] and oxidation of organic sulfides to sulfoxides, has stimulated the study of coordination chemistry of vanadium with multidentate ligands.[6–10] Several vanadium complexes have been shown to be active as insulin mimetics in vitro and in vivo, and [$V^{IV}O$(ethylmaltolato)$_2$] has passed phase I and II clinical tests,[11,12] demonstrating the usability of coordinating compounds of vanadium for the treatment of diabetes mellitus in humans.

The intestinal protozoan parasite *Entamoeba histolytica* has the capacity to invade intestinal mucosa, resulting in intestinal amoebiasis. Around 50 million people also suffer from liver abscess caused by *E. histolytica*, resulting in 50000–100000 deaths yearly.[13] Amoebiasis is the second leading cause of death among parasite diseases.[14] For the treatment of amoebiasis, metronidazole has been the drug of choice, but recent studies have shown that this drug has several toxic effects such as genotoxicity, gastric mucus irritation and spermatozoid damage.[15–17] Furthermore, failures in the treatment of several intestinal protozoan parasites may result from drug-resistant parasites.[18,19] Therefore, there is therapeutic demand for research on new drugs for treatment. Metal ions are known to often accelerate drug action, and the efficacy of a therapeutic agent may be enhanced upon coordination with a metal ion.[20] Vanadium complexes show a variety of biological properties, and oxidovanadium(IV) complexes have been used to prevent and improve dexamethasone-induced insulin resistance in 3T3-L1 adipocytes.[21] These compounds have also been used in receptor-mediated signals[22] and as anticancer agents.[23,24] Recently, we have reported the antiamoebic activity of various vanadium complexes, which gave encouraging results in in vitro experiments.[25,26]

[a] Department of Chemistry, Indian Institute of Technology Roorkee,
Roorkee 247667, India
Fax: +91-1332-273560
E-mail: rkmanfcy@iitr.ernet.in
[b] Department of Chemistry, Jamia Milia Islamia, Jamia Nagar, New Delhi 100025, India
[c] Centro de Química Estrutural, Instituto Superior Técnico, TU Lisbon,
Av Rovisco Pais, 1049-001 Lisbon, Portugal
[d] School of Life Sciences, Jawaharlal Nehru University, New Delhi 110062, India

Supporting information for this article is available on the WWW under http://dx.doi.org/10.1002/ejic.200900677.

In this paper, we describe the synthesis and characterisation of dinuclear oxidovanadium(IV) and dioxidovanadium(V) complexes of hydrazones **I** and **II** derived from 5,5′-methylenebis(salicylaldehyde) [$CH_2(Hsal)_2$] and nicotinic acid hydrazide (nah) or isonicotinic acid hydrazide (inh) (Scheme 1). The catalytic activity is demonstrated considering the oxidation, by peroxide, of methyl phenyl sulfide and diphenyl sulfide using the oxidovanadium(IV) complexes as catalyst precursors. In addition, the haloperoxidase activity is confirmed as the dioxidovanadium(V) complexes are active in the oxidative bromination of salicylaldehyde. The dioxidovanadium(V) complexes have also been screened against HM1:1MSS strains of *Entamoeba histolytica*.

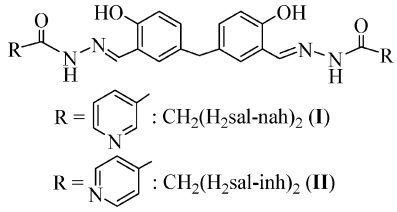

Scheme 1. Structures of ligands designated by **I** and **II** used in this work.

Results and Discussion

The reaction between [$V^{IV}O(acac)_2$] and $CH_2(H_2sal\text{-}nah)_2$ or $CH_2(H_2sal\text{-}inh)_2$ in a 2:1 ratio in refluxing methanol leads to the formation of dinuclear oxidovanadium(IV) complexes [$CH_2\{V^{IV}O(sal\text{-}nah)(H_2O)\}_2$] (**1**) and [$CH_2\{V^{IV}O(sal\text{-}inh)(H_2O)\}_2$] (**2**), respectively. These complexes exhibit normal magnetic moment values of 1.71 and 1.70 μ_B, respectively, indicating only very weak or possibly no magnetic exchange interaction between the two vanadium(IV) centres. Aerial oxidation of these complexes in the presence of KOH or $CsOH\cdot H_2O$ in methanol results in the formation of the corresponding salt of dioxidovanadium(V) species $[CH_2\{V^{V}O_2(sal\text{-}nah)\}_2]^{2-}$ and $[CH_2\{V^{V}O_2(sal\text{-}inh)\}_2]^{2-}$, respectively. Alternatively, these complexes can also be isolated directly by the aerial oxidation of in situ generated $V^{IV}O$ complexes in the presence of the corresponding hydroxide. Equations (1) and (2) present the whole synthetic procedure considering $CH_2(H_2sal\text{-}nah)_2$ as a representative ligand.

$$2\,[V^{IV}O(acac)_2] + CH_2(H_2sal\text{-}nah)_2 + 2\,H_2O \rightarrow [CH_2\{V^{IV}O(sal\text{-}nah)(H_2O)\}_2] + 4\,Hacac \quad (1)$$

$$[CH_2\{V^{IV}O(sal\text{-}nah)(H_2O)\}_2] + 2\,KOH + 1/2\,O_2 \rightarrow K_2[CH_2\{V^{V}O_2(sal\text{-}nah)\}_2]\cdot 2H_2O + H_2O \quad (2)$$

Complex $K_2[CH_2\{V^{V}O_2(sal\text{-}nah)\}_2]\cdot 2H_2O$ was also isolated by the reaction of potassium vanadate, generated in situ by dissolving V_2O_5 in an aqueous KOH solution, with the solution of the K^+ salt of **I** and adjustment of the pH of the reaction mixture to about 7.0 [Equation (3)]. Under similar reaction conditions the complex of ligand **II** always gave an emulsified mixture from which the desired complex could not be isolated.

$$2\,K[VO_3] + CH_2(HKsal\text{-}nah)_2 + 2\,H_2O \rightarrow K_2[CH_2\{V^{V}O_2(sal\text{-}nah)\}_2]\cdot 2H_2O + 2\,KOH \quad (3)$$

All complexes are soluble in methanol, ethanol, dmso and dmf. Scheme 2 presents the structures proposed for these complexes, which are supported by the spectroscopic characterisation (IR, electronic, ^1H, ^{13}C and ^{51}V NMR, and EPR), elemental analyses and thermogravimetric patterns. The coordination of the dianionic ligands involves their enolate tautomeric form (ONO^{2-}) (cf. Scheme 1).

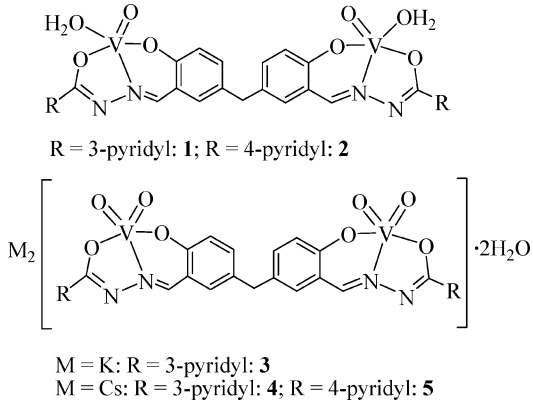

Scheme 2. Schematic structure of the $V^{IV}O$ and $V^{V}O_2$ complexes prepared.

Electronic Spectral Studies

Electronic spectroscopic data of ligands and complexes are presented in Table 1. Ligands **I** and **II** exhibit four absorption bands at about 216, 243, 294 and 341 nm that are assigned to $\phi \rightarrow \phi^*$, $\pi \rightarrow \pi_1^*$, $\pi \rightarrow \pi_2^*$ and $n \rightarrow \pi^*$ transitions, respectively. In complexes, these bands are generally shifted towards lower wavelengths. In addition, a new band of medium intensity appears at 407–414 nm, which is assigned to a ligand-to-metal charge transfer (LMCT) band. The band at 565 nm, observed at higher concentration for complexes **1** and **2**, is assigned to a d–d transition. For complexes **3**–**5** no such bands were detected.

Table 1. Electronic spectroscopic data of compounds.

Compounds	λ [nm]
$CH_2(H_2sal\text{-}nah)$ (**I**)	341, 294, 243, 216
$CH_2(H_2sal\text{-}inh)$ (**II**)	342, 294, 244, 217
$[CH_2\{V^{IV}O(sal\text{-}nah)(H_2O)\}_2]$ (**1**)	565, 408, 325, 242, 207
$K_2[CH_2\{V^{V}O_2(sal\text{-}nah)\}_2]\cdot 2H_2O$ (**3**)	408, 323, 292, 242
$Cs_2[CH_2\{V^{V}O_2(sal\text{-}nah)\}_2]\cdot 2H_2O$ (**4**)	408, 325, 288, 240, 206
$[CH_2\{V^{IV}O(sal\text{-}inh)(H_2O)\}_2]$ (**2**)	565, 407, 328, 282, 239
$Cs_2[CH_2\{V^{V}O_2(sal\text{-}inh)\}_2]\cdot 2H_2O$ (**5**)	414, 327, 283, 234

IR Spectral Studies

The IR spectroscopic data of ligands and complexes are presented in Table 2 (see also the Supporting Information).

Table 2. IR spectra of compounds [cm^{-1}].

Compounds	ν(C=O)	ν(C–O)	ν(C=N)	ν(V=O)	ν(N–N)
$CH_2(H_2sal\text{-}nah)$ (**I**)	1655	–	1617	–	961
$CH_2(H_2sal\text{-}inh)$ (**II**)	1653	–	1617	–	968
$[CH_2\{V^{IV}O(sal\text{-}nah)(H_2O)\}_2]$ (**1**)	–	1278	1594	983	1056
$K_2[CH_2\{V^{V}O_2(sal\text{-}nah)\}_2]\cdot 2H_2O$ (**3**)	–	1283	1597	926, 950	1029
$Cs_2[CH_2\{V^{V}O_2(sal\text{-}nah)\}_2]\cdot 2H_2O$ (**4**)	–	1278	1597	921, 950	1033
$[CH_2\{V^{IV}O(sal\text{-}inh)(H_2O)\}_2]$ (**2**)	–	1287	1593	987	1034
$Cs_2[CH_2\{V^{V}O_2(sal\text{-}inh)\}_2]\cdot 2H_2O$ (**5**)	–	1286	1593	927, 950	1066

The IR spectra of the ligands show bands at 1655 and 3204 [$CH_2(H_2sal\text{-}nah)_2$, **I**] and 1653 and 3250 cm^{-1} [$CH_2(H_2sal\text{-}inh)_2$, **II**] because of ν(C=O) and ν(N–H) stretches, respectively. This is indicative of their ketone nature in the solid state. Both bands disappear upon complex formation, indicating the enolisation and dissociation of H^+ induced by the metal ion. Other changes observed upon complex formation are as expected, namely the ligand band appearing at 961 (in **I**) and 968 cm^{-1} (in **II**) because the ν(N–N) stretch undergoes a blueshift of 95–98 cm^{-1}. This high-frequency shift of the ν(N–N) band is expected because of the decreased repulsion between the lone pairs of adjacent nitrogen atoms.[27]

All dioxidovanadium(V) complexes exhibit one sharp band in the 921–927 cm^{-1} region and one weak band at about 950 cm^{-1} due to ν_{sym}(O=V=O) and ν_{asym}(O=V=O) stretches. The O atoms of the $V^{V}O_2$ units are probably involved in binding to K^+/Cs^+ in the crystal structure; such oxygen coordination has been confirmed in anionic dioxidovanadium(V) complexes.[28,29] Oxidovanadium(IV) complexes display only one sharp band each at 983–987 cm^{-1} because of the ν(V=O) stretch.

^{1}H and ^{13}C NMR Studies

^{1}H NMR spectra of the ligands and complexes were recorded to obtain further evidence for the coordinating mode of ligands. The relevant data are presented in Table S1. The ^{1}H NMR spectra of ligands exhibit signals at δ = 10.84 (**I**) and at δ = 10.85 (**II**) due to the –NH proton, indicating their existence in the ketone form. The absence of these signals in V^{V} complexes is in agreement with enolisation and the subsequent replacement of H by the metal ion. Similarly, the absence of the signal for the phenol OH group ($\delta \approx$ 12.25 ppm in the ligands) indicates the coordination of the phenolate oxygen atom. A significant downfield shift of the azomethine (–CH=N–) proton signal in V^{V} complexes, as compared with the corresponding free ligands, also indicates the coordination of the azomethine nitrogen atom. This and the other ^{1}H NMR spectroscopic data are thus consistent with the ONO dibasic tridentate binding mode of each unit of ligands and in agreement with the conclusions drawn from IR data.

The ^{13}C NMR spectra recorded for complexes **3**–**5** contain 13 signals corresponding to the 27 carbon atoms of the molecules owing to their symmetry. The peaks observed and their assignments are included in the Supporting Information (Table S2), being compatible with the structures proposed.

Solution Behaviour of $K_2[CH_2\{V^{V}O_2(sal\text{-}nah)\}_2]\cdot 2H_2O$ (3)

The ^{51}V NMR spectrum of $K_2[CH_2\{V^{V}O_2(sal\text{-}nah)\}_2]\cdot 2H_2O$ (**3**) dissolved in MeOH has a resonance at δ = –538 ppm and a minor one at δ = –545 ppm (Figure 1a). In dmso a single peak is obtained at δ = –533 ppm [Figure 2A(a)]. The assignment of these and other resonances was done by also considering the experiments described below.

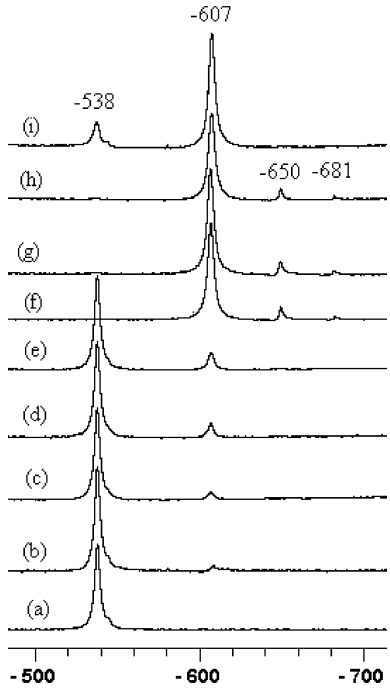

Figure 1. ^{51}V NMR spectra for solutions (about 4 mM) of $K_2[CH_2\{V^{V}O_2(sal\text{-}nah)\}_2]\cdot 2H_2O$ (**3**): (a) in MeOH and (b–h) after stepwise additions of an aqueous solution of 30% H_2O_2; (b) 0.5 equiv. H_2O_2 added; (c) 2 equiv. H_2O_2 (total) added; (d) 4.0 equiv. H_2O_2 (total) added; (e) 6.0 equiv. H_2O_2 (total) added; (f) 8.0 equiv. H_2O_2 (total) added; (g) 10 equiv. H_2O_2 (total) added; (h) solution of (g) after 2 h leaving tube open; (i) solution of (h) after 36 h leaving tube open.

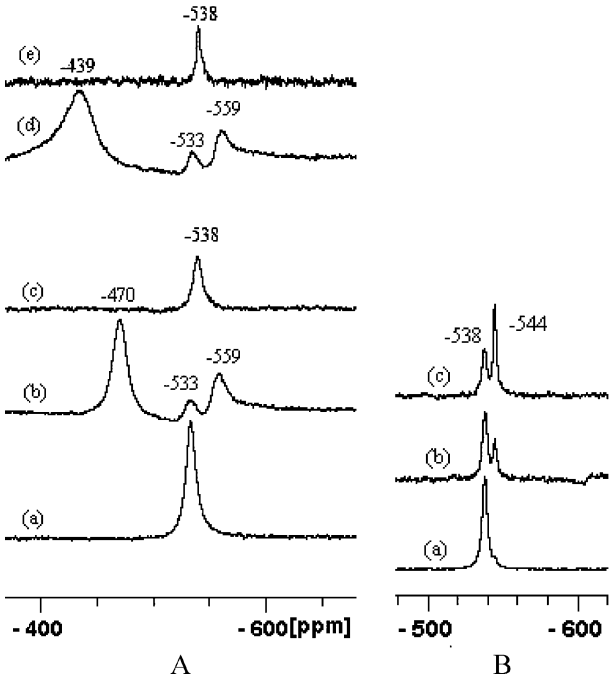

Figure 2. ^{51}V NMR spectra for $K_2[CH_2\{V^VO_2(sal\text{-}nah)\}_2]\cdot 2H_2O$ (**3**). (A): (a) in dmso (about 4 mM), (b) solution of (a) after addition of 3.0 equiv. of an aqueous solution of $HClO_4$ (15.8 M), the pH being about 3.1; (c) solution of (b) after addition of MeOH, the solution now containing equal volumes of dmso and MeOH; (d) solution of (a) after addition of 3.0 equiv. of an aqueous solution of HCl (11.6 M), the pH being about 3.3; (e) solution of (d) after addition of MeOH, the solution now containing equal volumes of dmso and of MeOH. (B): ^{51}V NMR spectra of **3** (a) in MeOH, about 4 mM; (b) after addition of 2.0 equiv. of an aqueous solution of HCl (11.6 M); (c) solution of spectrum (b) after standing for about 15 h.

Addition of methanol to a 4 mM solution of **3** in dmso shifts the δ = –533 ppm resonances to δ = –538 ppm, identical to the spectrum of **3** in MeOH only. The signal at δ = –538 ppm is assigned to $[CH_2\{VO_2(sal\text{-}nah)(MeOH)\}_2]^{2-}$ (**CII**, S = MeOH) in Scheme 3.[30,31]

Addition of acid ($HCl/HClO_4$), viz. 1, 2, 3, 4 equiv., to a methanolic solution of **3** leads to a decrease in intensity of the δ = –538 ppm peak and an increase at the δ = –545 ppm peak (see Figure 2B); the colour of the solution turns to red and the pH is about 2.5–3.3. The addition of acid may protonate the ligand so the δ = –545 ppm band may either be due to **CII** (S = H_2O) or to free vanadate (V_1). As addition of H_2O to the 4 mM solution of **3** in dmso shows an upfield shift to δ = –539 ppm, this indicates the involvement of the solvent molecule; we assign the δ = –539 ppm signal of Figure 2B to $[CH_2\{V^VO(sal\text{-}nah)(H_2O)\}_2]^{2-}$ (**CII**, S = H_2O).

Upon the stepwise addition of an aqueous 30% solution of H_2O_2 to the methanolic solution of **3** (about 4 mM) the resonance at δ = –538 ppm progressively disappears, and resonances at δ = –607 ppm are observed (Figure 1), which we tentatively assign to $[CH_2\{V^VO(O_2)(sal\text{-}nah)\}_2]^{2-}$ (**CIII**). Upon further stepwise additions of H_2O_2 (8 equiv. or more) the resonance at δ = –538 ppm totally disappears, and two new signals are detected at δ = –651 and –683 ppm, which we assign to inorganic peroxidovanadates {tentatively $[V^VO(O_2)]^+$ (**CIV**)[32] and $[V^VO(O_2)_2(H_2O)]^-$ (**CV**)}[33–39] (see Scheme 3). Leaving the NMR tube open for 36 h after recording the spectrum of Figure 1h, spectrum (i) was obtained, indicating the reversibility of the process.

The behaviour of **3** dissolved in dmso differs from what was observed in methanol (Figure 2). Upon addition of 3 equiv. $HClO_4$ the ^{51}V NMR spectrum shows two new signals at δ = –470 (br.) (about 86%) and –559 (about 9%) ppm, as well as the original resonance at δ = –533 (about 5%) ppm [Figure 2A(b), pH ≈ 3.1]. Similarly, addition of 3 equiv. of HCl to the solution of **3** in dmso yields two new signals at δ = –439 (br.) (about 82%) and –559 (about 14%) ppm, as well as the original resonance at δ = –533 (about 4%) ppm [Figure 2A(d)]. Similar results were obtained upon addition of H_2SO_4 instead of HCl or $HClO_4$.

For further investigation both solutions of (b) and (d) in Figure 2A were divided into three parts. On addition of MeOH to one of these only the peak at δ = –538 ppm [Figure 2A(e)] was detected, and this can be assigned to species **CII** (S = MeOH). Addition of 4 equiv. of KOH to the second portion yielded a resonance at δ = –533 ppm, indicating the reversibility of the reaction. The third portion of this solution was kept at room temperature for 48 h and then showed a major resonance at δ = –539 ppm corresponding to **CII**.

We assign the δ = –559 ppm lower-field resonances of Figure 2A(b) and (d) to the oxido/hydroxido species (**CVI**). The partial protonation of the ligand is also a plausible possibility (see below).

Additionally, the spectra of Figure 2A(b) and (d) show a global decrease and broadening of the ^{51}V NMR signals, indicating the presence of an oxidovanadium(IV) species in the solution, and this was confirmed by recording the EPR spectra for both solutions. The spectra are reasonably intense, and the spin Hamiltonian parameters obtained are both similar to those of solutions of **1** in dmso (see below) indicating an O_3N binding mode around the vanadium centre, that is, a binding mode identical to that of **1**.

To explain the peaks at $\delta \approx$ –440/–475 ppm, because of a V^V species, we now consider three possibilities: (i) the formation of a mixed-valence $V^{IV}O$–O–V^VO complex (see structure **CVII** in Scheme 3), (ii) a complex formulated as $[CH_2\{V^VO_2(sal\text{-}nah)\}\{V^{IV}O(sal\text{-}nah)\}]$ (see structure **CVIII**) or (iii) the formation of a V^VO–O–V^VO complex (see structure **CIX**), along with a V^{IV} complex, which corresponds to **1**. The ^{51}V NMR peaks in assignments (i) or (ii) correspond to the V^V-"half-part" of the molecule.

If a $V^{IV}O$–O–V^VO complex such as that represented in structure **CVII** is formed, the V–O–V angle should not be close to 180°, so that the unpaired electron is localised on one of the V atoms of the V–O–V dinuclear unit. To the best of our knowledge there is no previous example of ^{51}V NMR signals being obtained for $V^{IV}O$–O–V^VO complexes (or reports of attempts to measure them). In order that the δ = –440/–475 ppm resonances may be assigned to the V^VO_2-"half-part" of a species such as structure **CVIII**,

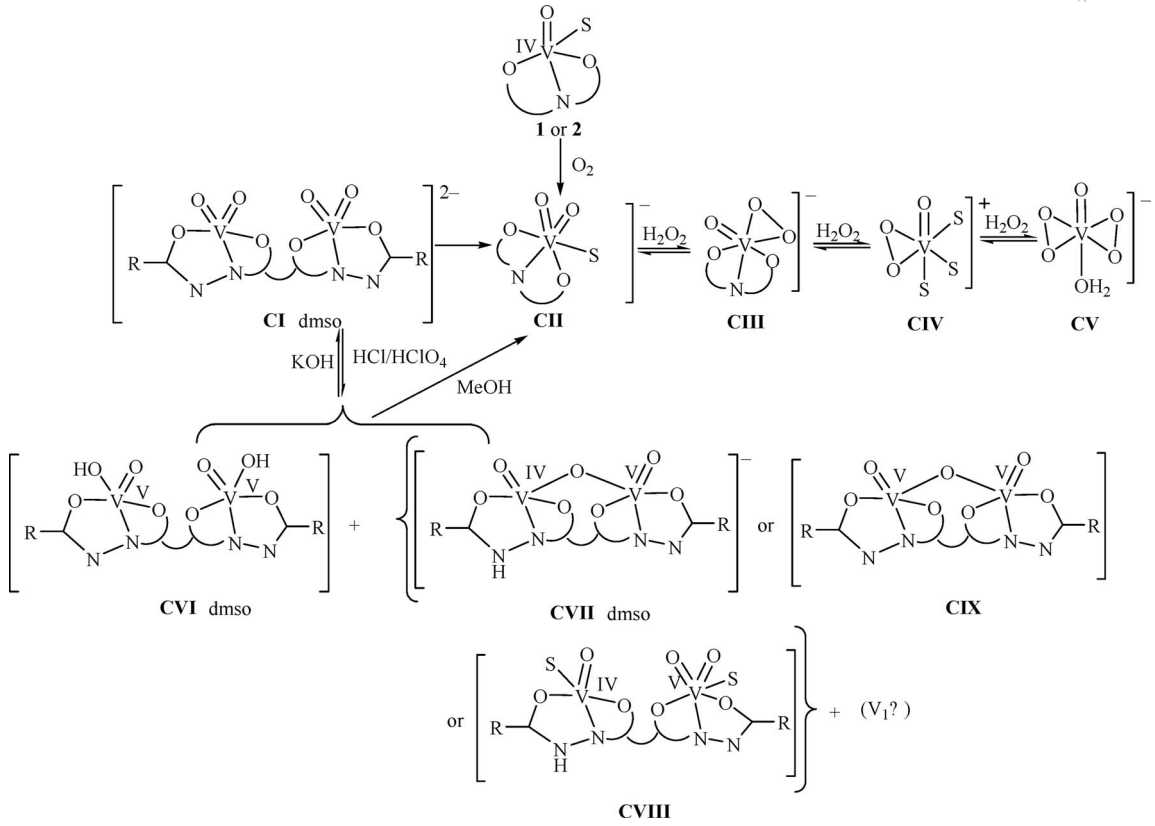

Scheme 3. Summary of speciation of vanadium species in solution.

which correspond to significantly deshielded V^V species, some electron density should have also been delocalised from the V^{IV} to the V^V centre, and it is not clear if this is feasible in **CVIII**. Globally, we consider structure **CIX** as a reasonable hypothesis of assignment for the δ = –440/–475 ppm resonances; the different values recorded possibly result from some electrostatic influence of the counterions present (Cl^-, ClO_4^- or SO_4^{2-}) nearby.

The formation of $[CH_2\{V^VOL\}_2]$ complexes, containing the V^VO^{3+} moiety, upon addition of acid, as reported for a few vanadium systems {e.g., salen and EHGS, ethylenebis[(*o*-hydroxyphenyl)glycine]},[40,41] could also be a possible explanation of the ^{51}V NMR signal appearing at $\delta \approx$ –444 to –466 ppm. However, no strong CT band was observed in the 500–600 nm range for complexes with our ligands **I** and **II** (see below) as was found in the salen and EHGS systems, so we assume these high-field resonances are not due to the formation of V^VOL-type complexes.

Solution Behaviour of $Cs_2[CH_2\{V^VO_2(sal\text{-}nah)\}_2]\cdot 2H_2O$ (4)

Similar to **3**, complex **4** dissolved in MeOH shows two resonances at δ = –537 and –544 ppm [Figure 3(a)], but the latter signal is more intense than the corresponding one in **3**. The major signal at δ = –537 ppm is assigned to $[CH_2\{VO_2(sal\text{-}nah)(MeOH)\}_2]^{2-}$ (**CII**, S = MeOH), and the minor one is probably vanadate (V_1) or a complex resulting from protonation of the coordinated N atom.[42,43] Upon stepwise addition of 30% H_2O_2 (up to 8 equiv.) resonances at δ = –606 and –649 ppm are recorded, which we assign to **CIII** and **CIV**, respectively (Scheme 3). Leaving the solution of Figure 3(f) in contact with air, spectrum (g) of Figure 3 was obtained after about 36 h, indicating that the reactions are reversible. Addition of acid (HCl or $HClO_4$, e.g., 2 equiv.) to a methanolic solution of **4** (see Figure S1) leads to a decrease in intensity of the δ = –538 ppm peak and an increase at δ = –545 ppm. This may be due either to protonation of the ligand, or to generation of **CII** (S = H_2O) or to free vanadate (V_1).

In dmso, complex **4** gives a resonance at $\delta \approx$ –532 ppm [Figure 4(a) or (d)]. Addition of methanol and water yielded the upfield resonances at δ = –537 and –538 ppm, respectively, confirming the involvement of solvent molecules in these **CII** species. Upon addition of 2 equiv. of concentrated HCl solution, two new resonances at δ = –444 (about 35%) and –559 (about 25%) ppm appear along with the original resonance at δ = –532 (about 30%) ppm. A similar behaviour was observed upon addition of 2 equiv. of $HClO_4$ (or H_2SO_4). A broadening of the bands also occurs, and rather intense EPR spectra could be recorded with the solutions of Figure 4(b) and (d) confirming the formation of $V^{IV}O$ complexes. The upfield resonance is assigned to the formation of an hydroxidooxidovanadium(V) species at δ = –559 ppm. Addition of 4 equiv. of KOH to the solutions of Figure 4(b) and (d) yielded only the resonance at δ = –532 ppm, corresponding to **4** in dmso, confirming the reversibility of the reaction. Addition of methanol to the solutions of Figure 4(b) and (d) yielded resonances at δ =

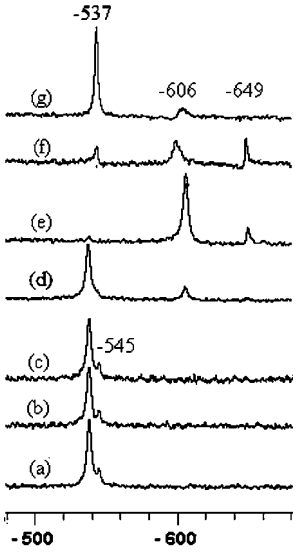

Figure 3. ^{51}V NMR spectra for $Cs_2[CH_2\{V^VO_2(sal\text{-}nah)\}_2]\cdot 2H_2O$ (**4**): (a) in MeOH (about 4 mM of **4**) and upon stepwise addition of aqueous 30% solution H_2O_2; (b) 1.0 equiv. H_2O_2; (c) 4.0 equiv. H_2O_2; (d) 6.0 equiv. H_2O_2; (e) 8.0 equiv. H_2O_2; (f) solution of (e) after 24 h leaving the tube open; (g) solution of (e) after 36 h of leaving the tube open.

–539 ppm corresponding to the dioxido species (**CII**, S = MeOH). The EPR spectra of the solutions of Figure 4(b) and (d) were simulated,[44] and the data indicate that the binding mode of the $V^{IV}O$ species present is identical to that of complex **1** in dmso (see below). The broad downfield

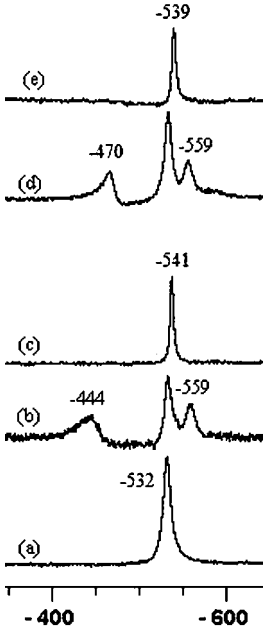

Figure 4. ^{51}V NMR spectra for $Cs_2[CH_2\{V^VO_2(sal\text{-}nah)\}_2]\cdot 2H_2O$ (**4**): (a) in dmso and after additions of aqueous acids: (b) 2.0 equiv. HCl and (d) 2.0 equiv. $HClO_4$. Upon addition of MeOH to the solutions of spectra (b) and (d) so that the mixtures contain equal volumes of MeOH and dmso, spectra (c) and (e), respectively, were recorded.

resonance is assigned as in the case of complex **3** (see Scheme 3 and the above discussion regarding structures **CVII**–**CIX**).

Solution Behaviour of $Cs_2[CH_2\{V^VO_2(sal\text{-}inh)\}_2]\cdot 2H_2O$ (5)

Similarly to the previous observations with **3** and **4**, the ^{51}V NMR spectrum of $Cs_2[CH_2\{V^VO_2(sal\text{-}inh)\}_2]\cdot 2H_2O$ (**5**) dissolved in MeOH (Figures S2a and S3a) shows signals at δ = –539 and –545 ppm, assigned to **CII** (S = MeOH and H_2O) and free vanadate. Upon addition of aqueous solutions of either HCl or $HClO_4$ (2 equiv. of acid) a peak at δ = –545 ppm was detected, which may at least partly correspond to vanadate (Figure S3). Formation of the peroxido complexes **CIII** and **CIV** (δ = –606 and –649 ppm, respectively) was confirmed upon addition of an aqueous solution of 30% H_2O_2 (1, 2 and 10 equiv.) (Figure S2). In dmso (Figure S4) the behaviour is similar to what was recorded for complexes **3** and **4**.

EPR and UV/Vis Study

The EPR spectra of "frozen" solutions (77 K) in dmso of complexes **1** and **2** are depicted in Figure 5. Two sets of eight-line spectra showing hyperfine splitting due to the ^{51}V nucleus are obtained, characteristic of square-pyramidal complexes with an axially compressed d^1_{xy} configuration. The spectra were simulated, and the spin Hamiltonian parameters obtained[44] are included in Table 3.

The value of $A_\parallel$ can be calculated by using the additivity relationship [$A_\parallel^{est} = \Sigma A_{\parallel,i}$ (i = 1–4)] proposed by Wurthrich[45] and Chasteen,[46] with estimated accuracy of $\pm 3\times10^{-4}$ cm^{-1}. The $A_\parallel$ values obtained for **1** and **2** (Table 3) agree with the values calculated from the partial contributions of the equatorial donor groups: H_2O (45.7×10^{-4} cm^{-1}), $O_{phenolate}$ (38.9×10^{-4} cm^{-1}), N_{imine}, (38.1×10^{-4} to 43.7×10^{-4} cm^{-1}), O-enolate$^{(1-)}$ (37.6×10^{-4} cm^{-1}), O_{dmso} (41.9×10^{-4} cm^{-1}) and O_{MeOH} (45.7×10^{-4} cm^{-1}).[47,48]

The EPR spectra of both complexes in dmso are in good agreement with an O_3N binding mode, one of the equatorial donor atoms being O_{dmso}. The effect of solvent on EPR parameters was examined by also measuring the spectra in MeOH (e.g., Figure 6). As indicated in Table 3 for **1**, the $g_\parallel$ value decreases from 1.951 to 1.948, and $A_\parallel$ increases from 163.3 to 166.4, this being compatible with the substitution of one coordinated O_{dmso} by an O_{MeOH} atom.[48] Similar data were obtained for **2** (Table 3).

Addition of H_2O_2 portions to solutions of **1** or **2** in MeOH acidifies the solutions, and different $V^{IV}O$ species form with EPR parameters $g_\parallel$ = 1.936, $A_\parallel = 177.8\times10^{-4}$ cm^{-1} for **1** and $g_\parallel$ = 1.935, $A_\parallel = 178.0\times10^{-4}$ cm^{-1} for **2**; the $V^{IV}O$ is also progressively oxidised to V^V (Figures S5 and S6). According to the $g_\parallel$ and $A_\parallel$ values obtained for these partially oxidised solutions, in these $V^{IV}O$ species the binding mode is probably O_4, the $V^{IV}O$ complexes being extensively hydrolysed.

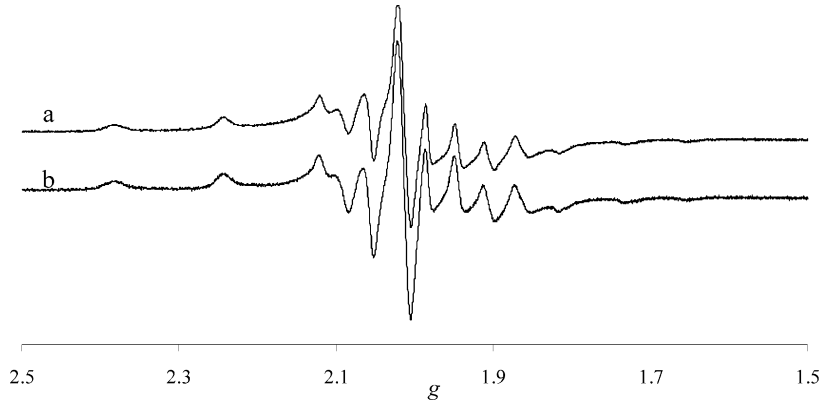

Figure 5. EPR spectra of frozen solution (4 mM) samples of $[CH_2\{V^{IV}O(sal\text{-}nah)(H_2O)\}_2]$ (**1**) (a) and $[CH_2\{V^{IV}O(sal\text{-}inh)(H_2O)\}_2]$ (**2**) (b) in dmso.

Table 3. Spin Hamiltonian parameters obtained by simulation[44] of the experimental EPR spectra recorded for dmso solutions of complexes **1** and **2** at 77 K.

Complex	Solvent	$g_{\parallel}$	$A_{\parallel} \times 10^4$ [cm^{-1}]	$g_{\perp}$	$A_{\perp} \times 10^4$ [cm^{-1}]
$[CH_2\{V^{IV}O(sal\text{-}nah)(H_2O)\}_2]$ (**1**)	dmso	1.951	163.3	1.980	56.7
	MeOH	1.948	166.4	1.979	57.5
0.5 equiv. H_2O_2	MeOH	1.936	177.8	1.977	66.0
$[CH_2\{V^{IV}O(sal\text{-}inh)(H_2O)\}_2]$ (**2**)	dmso	1.951	162.3	1.981	56.8
	MeOH	1.949	165.9	1.979	57.4
0.5 equiv. H_2O_2	MeOH	1.935	178.0	1.977	66.2

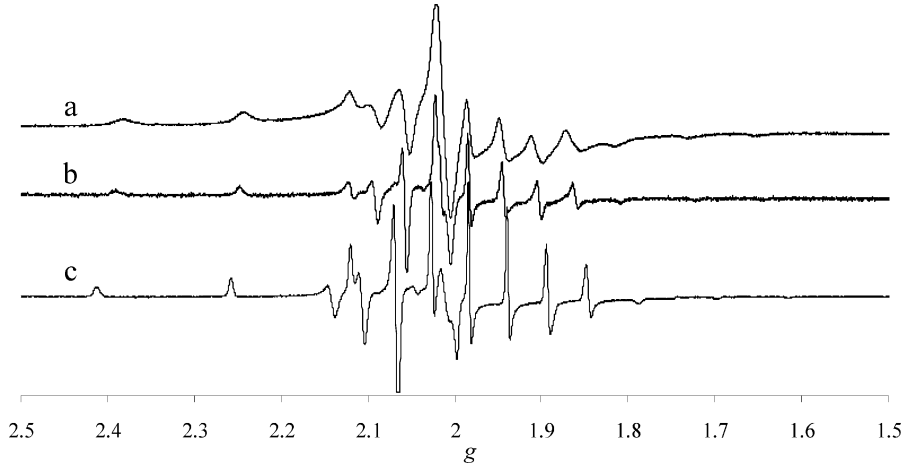

Figure 6. First-derivative EPR spectra (at 77 K) of a solution of $[CH_2\{VO(sal\text{-}nah)(H_2O)\}]_2$ (**1**): (a) in dmso (about 4 mM); (b) after addition of an equal volume of MeOH; and (c) after addition of 0.5 equiv. of an aqueous 30% H_2O_2 solution.

Upon leaving solutions of **1** or **2** in dmso in contact with air, after about 3–4 d ^{51}V NMR resonances were recorded at $\delta \approx -532$ ppm (Figure S6). V^VO_2 complexes therefore form with signals similar to those recorded for dmso solutions of **3**–**5**. With the stepwise addition of aqueous H_2O_2 solution (1, 2, 3, 4, 5 equiv.) peaks at $\delta \approx -597$ and –648 ppm were obtained, corresponding to the peroxido complexes **CIII** and **CIV**, respectively. Subsequent addition of 10 equiv. of methyl phenyl sulfide produced, after about 12 h, the resonance at $\delta = -539$ ppm, corresponding to a dioxido species (**CII**, S = MeOH), supporting the reversibility of the processes.

The formation of peroxido complexes in methanol by treatment of the respective dioxido complexes with H_2O_2 could also be established by electronic absorption. Thus, the addition of 30% aqueous H_2O_2 (30 drops, 18.04 mmol) to 20 mL of an approximately 4.135×10^{-5} M solution of $Cs_2[CH_2\{V^VO_2(sal\text{-}inh)\}_2]\cdot 2H_2O$ (**5**) and recording of the spectral changes after every 25 min resulted in the spectra presented in Figure 7. The band at 412 nm slowly shifted to 415 nm along with a decrease in intensity. The two UV bands appearing at 232 and 282 nm (not within the scale of the figure) increase in intensity, whereas the 328 nm band becomes a shoulder. A band at about 470 nm slightly in-

creases its intensity. This change in spectra is interpreted as the formation of a peroxido compound. Similar spectral changes were recorded with solutions of **3** and **4** upon similar treatment (Figures S7 and S8).

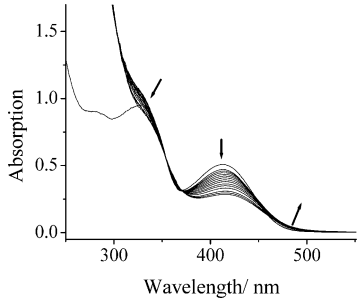

Figure 7. UV/Vis spectrum of 20 mL of an approximately 4.135×10^{-5} M methanolic solution of $Cs_2[CH_2\{V^VO_2(sal\text{-}inh)\}_2]\cdot 2H_2O$ (**5**) and spectral changes observed with time after addition of 30% aqueous H_2O_2 (30 drops, 18.04 mmol). Each spectrum was recorded at 25-min intervals.

The reactivity of methanolic solutions of dioxidovanadium(V) complexes with HCl was also monitored by electronic absorption spectroscopy. Thus, the dropwise addition of HCl gas saturated in methanol to 20 mL of a 6.535×10^{-5} M solution of $Cs_2[CH_2\{V^VO_2(sal\text{-}inh)\}_2]\cdot 2H_2O$ (**5**) caused the darkening of the solution along with an increase in intensity of the 279 nm band and its transformation into a shoulder (Figure 8). The other UV bands at 274 and 298 nm only gained intensity. The band appearing at 412 nm apparently progressively broadened with decrease in its intensity, whereas the band at about 470 nm increased in intensity. Very similar features have been observed with **3** and **4** upon similar treatment (Figures S9 and S10).

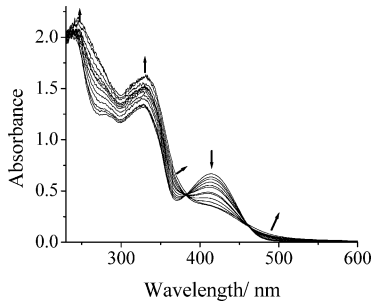

Figure 8. Spectral changes obtained during titration of 20 mL of a 6.535×10^{-5} M methanolic solution of $Cs_2[CH_2\{V^VO_2(sal\text{-}inh)\}_2]\cdot 2H_2O$ (**5**) with HCl gas saturated in methanol; the spectra were recorded after the successive additions of one-drop portions.

As done by other authors for other systems,[34,49–51] we interpret these results in terms of the formation of an oxido/hydroxido species $[CH_2\{VO(OH)(L)\}_2]$. It is also possible that the ligand might become protonated, complexes $[CH_2\{VO_2(HL)(S)\}_2]$ being formed. Protonation of the hydrazone nitrogen atom has been reported, for example, for the structurally characterised complex [VO(Hsal-bhz)] (H_2sal-bhz derives from salicylaldehyde and benzoyl hydrazide), which forms on treatment of the corresponding anionic dioxido complex with HCl,[42] as well as for complex [VO(salim)(acac)] (salim = a Schiff base ligand also containing imidazole), where the EPR and ESEEM spectra recorded upon addition of acid were explained by the protonation of the imine N atom.[43]

Catalytic Activity Studies

Oxidation of Methyl Phenyl Sulfide and Diphenyl Sulfide

It is known that several vanadium-dependent haloperoxidases also catalyse sulfoxidations.[47,52,53] We tested complexes $[CH_2\{V^{IV}O(sal\text{-}nah)(H_2O)\}_2]$ (**1**) and $[CH_2\{V^{IV}O(sal\text{-}inh)(H_2O)\}_2]$ (**2**) as catalyst precursors, taking methyl phenyl sulfide and diphenyl sulfide to model these reactions using aqueous 30% H_2O_2 as oxidant. Between the two complexes studied, **1** was chosen as a representative one, and the amounts of catalyst precursor and oxidant were varied to obtain maximum conversion (based on substrate consumption). The effect of H_2O_2 was studied (Figure S11) by considering substrate/oxidant ratios of 1:1, 1:2 and 1:3 for the fixed amount of catalyst (0.015 g) and substrate (1.24 g, 10 mmol) in petroleum ether (10 mL), and the reaction was monitored at room temperature. Thus, in 7 h of contact time, on increasing the substrate/oxidant ratios from 1:1 to 1:2 the conversion increased from 11.4% to 99.6%. Increasing this ratio to 1:3 did not improve conversion except for the completion of the reaction within 6 h and a slight change in the selectivity of products.

Similarly, four different amounts of catalyst precursor, viz 0.005, 0.015, 0.025, 0.035 g, were taken at fixed reaction conditions optimised as above [i.e., substrate (1.24 g, 10 mmol), H_2O_2 (2.27 g, 20 mmol) and petroleum ether (10 mL)] to see the effect of amount of catalyst on the reaction, and the results are presented in Figure S12. It is clear from the figure that 0.015 g of catalyst was sufficient to give 99.6% conversion with a turnover frequency of 57.1 h^{-1}. A higher amount of catalyst only reduced the time taken to achieve the steady state of the reaction.

Therefore, from these experiments, the best reaction conditions for the maximum oxidation of methyl phenyl sulfide are considered to be: substrate (1.24 g, 10 mmol), catalyst (0.015 g), H_2O_2 (2.27 g, 20 mmol) and petroleum ether (10 mL). The other substrate (diphenyl sulfide) with **1** as catalyst precursor under the above reaction conditions, as well as the other catalyst precursor **2** for both substrates, was also tested, and the corresponding results are summarised in Table 4.

From Table 4, it is clear that more than 99% of methyl phenyl sulfide was converted into products using both catalysts, whereas diphenyl sulfide was only converted by 62.8–68.4% under the conditions used. Normally, two major products, sulfoxide and sulfone, were obtained in major yield along with only small amounts (<0.4%) of an unidentified product. The selectivity of the major product (sulfone) is about 85%, whereas that of sulfoxide is about 15% in all cases. In the absence of the catalyst, the reaction mixture gave 35.3% conversion of methyl phenyl sulfide with 65.5% selectivity towards sulfoxide, 34.2% towards

Table 4. Percent conversion[a] of methyl phenyl sulfide and diphenyl sulfide along with the turnover frequency and selectivity of the reaction products after 7 h of reaction time.

Entry	Catalyst	Substrate[b]	Conversion [%]	TOF [h^{-1}]	Selectivity [%]		
					Sulfoxide	Sulfone	Others
1	**1**	mps	99.6	62.6	16.8	82.5	0.2
2	**1**	dps	68.4	45.0	15.4	84.5	0.2
3	**2**	mps	99.2	62.4	13.3	86.3	0.4
4	**2**	dps	62.8	39.4	14.3	85.4	0.4

[a] Reaction conditions: substrate (10 mmol), catalyst (0.015 g), H_2O_2 (2.27 g, 20 mmol) and petroleum ether (10 mL), room temperature. [b] mps = methyl phenyl sulfide, dps = diphenyl sulfide.

sulfone and about 0.3% of an unidentified product. Blank reaction with diphenyl sulfide under the above reaction conditions gave about 5% conversion with a sulfoxide/sulfone selectivity of 57:43. Thus, catalysts not only improve the conversion of substrates, they alter the selectivity of the products as well.

The conversion of methyl phenyl sulfide and the selectivity of different reaction products with **1** as catalyst under the optimised reaction conditions have been analysed as a function of time and are presented in Figure 9. It is clear from the plot that the formation of methyl phenyl sulfoxide is good (75.6%) at the beginning but decreases considerably with time, being 16.8% after 7 h of reaction. The selectivity of methyl phenyl sulfone is 24.2% after 1 h of reaction time and reaches 83.0% after 7 h. The unidentified product, which is only in a minor amount, remains nearly constant throughout.

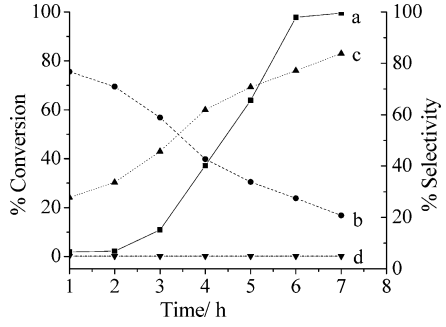

Figure 9. Conversion of methyl phenyl sulfide and variation in the selectivity of different reaction products as a function of time with **1** as catalyst: (a) conversion of methyl phenyl sulfide, (b) selectivity of methyl phenyl sulfoxide, (c) selectivity of methyl phenyl sulfone and (d) other unidentified product.

Oxidative Bromination of Salicylaldehyde

It is known that vanadium(V) complexes can also act as functional models of vanadium-dependent haloperoxidases, catalysing the oxidative bromination of organic substrates in the presence of H_2O_2 and bromide ion.[46,47,49,54] During oxidation, the vanadium complex reacts with 1 or 2 equiv. of H_2O_2, forming oxidomono(peroxido) $\{[CH_2\{V^VO(O_2)(L)\}_2]^{2-}$, **CIII**$\}$ or oxido(peroxido) $\{[V^VO(O_2)]^+$, **CIV**$\}$ or oxidobis(peroxido) (**CV**) species (vide supra). Species **CIII** (Scheme 3) or its protonated form ultimately oxidises bromide species (to Br_2, Br_3^- and/or HOBr), the bromination of the substrate then proceeding with the liberation of a proton.[50] We have found that the dioxidovanadium(V) complexes reported here satisfactorily catalyse the oxidative bromination of salicylaldehyde to give 5-bromosalicylaldehyde, 3,5-dibromosalicylaldehyde and 2,4,6-tribromophenol by using H_2O_2/KBr in the presence of $HClO_4$ in aqueous solution at room temp. (cf. Scheme 4).

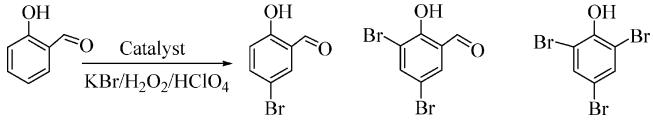

Scheme 4. Oxidation products of salicylaldehyde.

After several trials, the best suited reaction conditions obtained for the maximum conversion of salicylaldehyde in 7 h of reaction time were: salicylaldehyde (2.44 g, 20 mmol), KBr (5.95 g, 50 mmol), aqueous 30% H_2O_2 (13.62 g, 120 mmol), catalyst (0.020 g for **4** and **5** or 0.016 g for **3**),

Table 5. Conversion of salicylaldehyde and selectivity of oxidative brominated product data after 7 h of contact time.[a]

Entry	Catalyst	Substrate/H_2O_2 ratio	Conversion [%]	TOF [h^{-1}]	Selectivity of products		
					Monobromo	Dibromo	Tribromo
1	**5**	1:2	89.4	122	71.5	26.3	2.1
2	**5**	1:3	88.7	121	69.3	27.9	2.8
3	**5**	1:4	91.0	125	51.7	42.8	5.5
4	**5**	1:5	92.7	127	28.8	59.4	11.8
5	**5**	1:6	94.5	129	12.9	64.9	22.2
6	**3**	1:2	87.2	120	78.1	19.8	2.1
7	**3**	1:4	93.1	128	50.4	41.3	8.3
8	**4**	1:2	86.8	119	76.3	19.1	4.6
9	**4**	1:4	91.8	126	57.3	39.2	3.5

[a] Other reaction conditions: salicylaldehyde (2.44 g, 20 mmol), KBr (5.95 g, 50 mmol), catalyst (0.020 g for **4** and **5** or 0.016 g for **3**), aqueous 70% $HClO_4$ (11.44 g, 80 mmol) and water (40 mL).

aqueous 70% $HClO_4$ (11.44 g, 80 mmol) and water (40 mL); the addition of $HClO_4$, however, in four equal portions during the first 2 h of reaction time was necessary to improve the conversion of the substrate and to avoid decomposition of catalyst. Under the above conditions, a maximum of 89.4% conversion was achieved with $Cs_2[CH_2\{V^VO_2(sal\text{-}inh)\}_2]\cdot 2H_2O$ (**5**), and at least three products were identified (see Table 5). Increasing the amount of oxidant improves the conversion of salicylaldehyde. However, the selectivity of 5-bromosalicylaldehyde decreases considerably, whereas those of 3,5-dibromosalicylaldehyde and 2,4,6-tribromophenol increase. The presence of excess H_2O_2 facilitates the formation of more and more HOBr, which ultimately helps in the further oxidative bromination of salicylaldehyde in other position(s). Catalysts **3** and **4** gave very similar results. The counterions (Cs^+ or K^+) did not much affect the conversion. In the absence of the catalyst, the reaction mixture gave about 4% conversion of salicylaldehyde.

Mechanism of Bromination and Sulfide Oxidation

$Cs_2[CH_2\{V^VO_2(sal\text{-}nah)\}_2]\cdot 2H_2O$ (**4**), $Cs_2[CH_2\{V^VO_2(sal\text{-}inh)\}_2]\cdot 2H_2O$ (**5**) and $K_2[CH_2\{V^VO_2(sal\text{-}nah)\}_2]\cdot 2H_2O$ (**3**) were used as catalysts to carry out oxidative brominations, and a global outline of the reaction is presented in Scheme 5. The formation of intermediates proposed in the catalytic cycles, that is, hydroxidooxido complexes such as $[CH_2\{V^VO(OH)(L)\}_2]$ (**CVI**), oxidoperoxido complexes $[CH_2\{V^VO(O_2)(L)\}_2]^{2-}$ (**CIII**) and peroxido complex $[V^VO(O_2)]^+$ (**CIV**), were confirmed on the basis of ^{51}V NMR spectroscopy and characteristics in the UV/Vis spectra of the anionic dioxidovanadium precursor compounds $[CH_2\{V^VO_2(L)\}_2]^{2-}$ (**CI** or **CII**), treated with acid and hydrogen peroxide, which ultimately oxidise bromide, possibly through a hydroperoxido intermediate. The oxidised bromine species (Br_2, Br_3^- and/or HOBr) then brominate the substrate.[47,54,55]

Complexes $[CH_2\{V^{IV}O(sal\text{-}nah)(H_2O)\}_2]$ (**1**) and $[CH_2\{V^{IV}O(sal\text{-}nah)(H_2O)\}_2]$ (**2**) were used for sulfoxidations, and we tried to investigate the intermediate species by EPR and ^{51}V NMR spectroscopy. Upon titration with H_2O_2, complexes are oxidised and generate signals at δ = –538, –597 and –649 ppm [dioxido complex **CII**, peroxido complex **CIII**, peroxido **CIV** and bis(peroxido) **CV**]. The addition of sulfide consumes the intermediates formed and yields only one ^{51}V NMR signal, at δ = –539 ppm, corresponding to the dioxidovanadium(V) complex **CII**. This supports the involvement of these intermediate species during the catalytic process, namely the hydroperoxido form of **CIII**. The catalytic cycle for oxidation of methyl phenyl sulfide (as a model reaction), proposed previously by several authors,[55–57] is also given in Scheme 5.

Antiamoebic Activity

Dioxidovanadium (V) complexes along with ligands **I** and **II** were screened for antiamoebic activity in vitro against the HM1:IMSS strain of *E. histolytica*. The IC_{50} values are in the micromolar range and are shown in Table 6. The data are presented in terms of percentage growth inhibition related to untreated controls and plotted as percentage inhibition versus logarithm of the dose concentration. The IC_{50} values were obtained by interpolation in the corresponding dose response curves. Complexes $K_2[CH_2\{V^VO_2(sal\text{-}nah)\}_2]\cdot 2H_2O$ (**3**) (IC_{50} = 0.47 μM) and $Cs_2[CH_2\{V^VO_2(sal\text{-}inh)\}_2]\cdot 2H_2O$ (**5**) (IC_{50} = 0.32 μM) cause a marked inhibition, whereas ligands **I** (IC_{50} = 8.97 μM) and **II** (IC_{50} = 7.61 μM) are less active than metronidazole. This shows that complexation of the organic ligands to vanadium substantially enhances the activity. It is plausible that complexation directly or indirectly favours permeation of the complexes through the lipid layer of the cell membrane.[58] The significance of the statistical difference between the IC_{50} values of metronidazole and the most active complexes **3** and **5** was evaluated by a *t* test. The values of the calculated *t* were found to be higher than the table value of *t* at the 4% level,[59] thus clearly demonstrating that the vanadium complexes are potent inhibitors of the development of *E. histolytica* in vitro and that they are more active than the standard drug metronidazole.

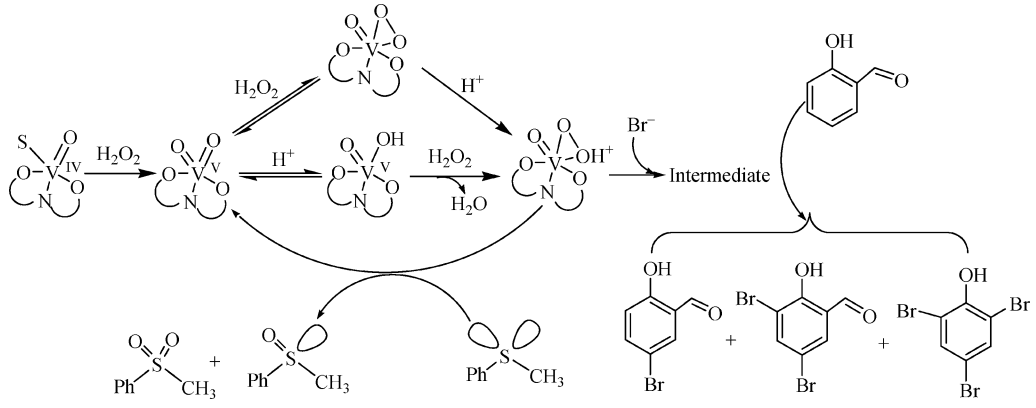

Scheme 5. Outline of the catalytic processes.

Table 6. Vanadium complexes, antiamoebic activity against HM1:IMSS strain of *E. histolytica* and toxicity profile of compounds **3** and **5**.

Entry	Compound	Antiamoebic		Toxicity profile	
		IC_{50} [μM][a]	S.D.[b]	IC_{50} [μM][a]	S.D.[b]
1	$CH_2(H_2sal\text{-}nah)_2$ (**I**)	8.97	0.01	N.D.	N.C.
2	$CH_2(H_2sal\text{-}inh)_2$ (**II**)	7.61	0.02	N.D.	N.C.
3	$K_2[CH_2\{V^VO_2(sal\text{-}nah)\}_2]\cdot 2H_2O$ (**3**)	0.47	0.01	150	0.045
4	$Cs_2[CH_2\{V^VO_2(sal\text{-}nah)\}_2]\cdot 2H_2O$ (**4**)	4.34	0.05	N.D.	N.C.
5	$Cs_2[CH_2\{V^VO_2(sal\text{-}inh)\}_2]\cdot 2H_2O$ (**5**)	0.32	0.03	50	0.015
6	Metronidazole	1.89	0.03	>750	0.050

[a] The values were obtained from at least three separate assays done in duplicate. [b] Standard deviation; N.D., not done; N.C., not calculated.

Toxicity of Compounds Assessed by the MTT Assay

The cells were treated with various concentrations of compounds **3** and **5** or vehicle (dmso) alone for 24, 48 and 72 h (as indicated in Figures 10 and 11). Cell survival was determined by an MTT assay. Cell viability was calculated as described in the Materials and Methods section, as the mean from three independent experiments in which each treatment was done in triplicate. To assess the survival effects of the compounds, human cervical (HeLa) cells were used; 6000 cells per well in 200 μL of complete DMEM medium were plated. Different concentrations of the different compounds were added to the wells as indicated in Figures 10 and 11. The concentration range for compound **3** was 0.47–250 μM/L and for compound **5** 0.32–250 μM/L. The viable cells were measured after 24, 48 and 72 h by MTT assay. At 72 h, the IC_{50} of compounds **3** and **5** are 150 and 50 μM/L, respectively. The cell survival assay was also performed in the presence of metronidazole and the IC_{50} value was found to be more than 750 μM, as given in Table 6. This shows that compounds **3** and **5** are more toxic than metronidazole.

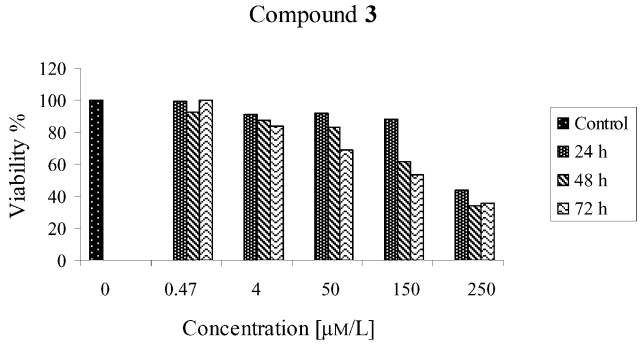

Figure 10. Percentage of viable cells after 24, 48 and 72 h on human cervical (HeLa) cells on incubation with various concentrations of compound **3** or vehicle (dmso). Cell survival was determined by the MTT assay.

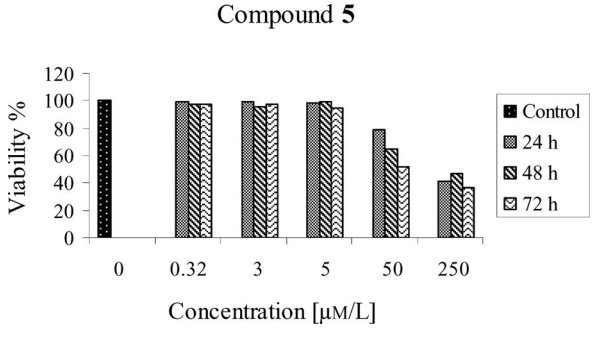

Figure 11. Percentage of viable cells after 24, 48 and 72 h on human cervical (HeLa) cells on incubation with various concentrations of compound **5** or vehicle (dmso). Cell survival was determined by the MTT assay.

Conclusions

The hydrazones $CH_2(H_2sal\text{-}nah)_2$ (**I**) and $CH_2(H_2sal\text{-}inh)_2$ (**II**) derived from 5,5′-methylenebis(salicylaldehyde) [$CH_2(Hsal)_2$] and nicotinic acid hydrazide (nah) or isonicotinic acid hydrazide (inh) and their $V^{IV}O$ and V^VO_2 complexes were synthesised and characterised. The complexes are dinuclear in the solid state and in solution, but no significant interactions are detected between the vanadium centres.

Compounds $[CH_2\{V^VO_2(sal\text{-}nah)\}_2]^{2-}$ and $[CH_2\{V^VO_2(sal\text{-}inh)\}_2]^{2-}$ were shown to be functional models of vanadium-dependent haloperoxidases, satisfactorily catalysing the oxidative bromination of salicylaldehyde to give 5-bromosalicylaldehyde, 3,5-dibromosalicylaldehyde and 2,4,6-tribromophenol by using H_2O_2/KBr in the presence of $HClO_4$ in aqueous solution at room temperature. The complexes $[CH_2\{V^{IV}O(sal\text{-}nah)(H_2O)\}_2]$ and $[CH_2\{V^{IV}O(sal\text{-}inh)(H_2O)\}_2]$ were shown to be catalyst precursors for the catalytic oxidation, by peroxide, of methyl phenyl sulfide and diphenyl sulfide, yielding the corresponding sulfoxide and sulfone at room temperature.

The reactivity in methanol and dmso of the $V^{IV}O$ and V^VO_2 complexes of $CH_2(H_2sal\text{-}nah)_2$ (**I**) and $CH_2(H_2sal\text{-}inh)_2$ (**II**) was studied by UV/Vis, EPR and ^{51}V NMR spectroscopy, by adding H_2O_2 or acid (HCl or $HClO_4$) or both. The formation of several species was established, some of them probably being intermediates in the catalytic processes studied, namely $[CH_2\{V^VO(O_2)(L)\}_2]^{2-}$ and $[CH_2\{V^VO(OH)(L)\}_2]$. On addition of acid (HCl or $HClO_4$) the V^V species present are partly reduced, yielding $V^{IV}O$ species containing the $\{V^{IV}O(sal\text{-}nah)(S)\}$ and $\{V^{IV}O(sal\text{-}inh)(S)\}$ moieties (S = solvent), the hydroxidooxido complex and a ^{51}V-NMR-active species whose nature is suggested.

Amoebiasis is caused by *Entamoeba histolytica*, the second leading cause of death among parasite diseases. For the treatment of amoebiasis metronidazole has been, until now, the drug of choice. The V^V complexes of $CH_2(H_2$sal-nah$)_2$ (**I**) and $CH_2(H_2$sal-inh$)_2$ (**II**) were also screened against HM1:1MSS strains of *Entamoeba histolytica*, the results showing that they are significantly more active than metronidazole. The MTT assay results showed that compounds **3** and **5** are not much toxic against human cervical (HeLa) cell lines.

Experimental Section

Materials: V_2O_5, isonicotinic acid hydrazide (Loba Chemie, India), nicotinic acid hydrazide (Fluka Chemie, GmbH, Switzerland), acetylacetone (Aldrich, USA), salicylaldehyde (Hsal), 30% aqueous H_2O_2 and 70% $HClO_4$ (Qualigens, India) were used as obtained. Other chemicals and solvents were of analytical reagent grade. $[V^{IV}O(acac)_2]$ was prepared according to the method reported in the literature.[60]

Characterisation Procedures: Elemental analyses of the compounds were carried out with an Elementar model Vario-El-III. IR spectra were recorded as KBr pellets with a Nicolet NEXUS Aligent 1100 series FTIR spectrometer. Electronic spectra were measured in methanol or dmf with a UV-1601 PC UV/Vis spectrophotometer. ^{1}H NMR spectra were obtained with a Bruker 200, and ^{13}C and ^{51}V NMR spectra with a Bruker Avance III 400 MHz spectrometer by using the common parameter settings. NMR spectra were usually recorded in [D$_4$]MeOD or [D$_6$]dmso, and $\delta(^{51}V)$ values are referenced relative to neat $VOCl_3$ as external standard. Thermogravimetric analyses of the complexes were carried out under oxygen by using a TG Stanton Redcroft STA 780 instrument. The magnetic susceptibilities were measured with a Vibrating Sample Magnetometer model 155 by using nickel as standard. Diamagnetic corrections were carried out by using Pascal's constants.[61] EPR spectra were recorded with a Bruker ESP 300E X-band spectrometer. The spin Hamiltonian parameters were obtained by simulation of the spectra with the computer program of Rockenbauer and Korecz.[44] A Thermax Nicolet gas chromatograph fitted with a HP-1 capillary column (30 m × 0.25 mm × 0.25 μm) and FID detector was used to analyse the reaction products, and their quantifications were made on the basis of the relative peak area of the respective product. The identity of the products was confirmed by using a GC–MS model Perkin–Elmer Clarus 500 and comparing the fragments of each product with the library available.

In Vitro Testing against *E. histolytica*: The ligands and their dioxidovanadium(V) complexes **3**–**5** were screened in vitro for antiamoebic activity against the HM1:1MSS strain of *E. histolytica* by using a microplate method.[62] *E. histolytica* trophozoites were cultured in TYIS-33 growth medium in a 96-well microtitre plate;[63] dmso (40 μL) was added to all the samples (1 mg) followed by enough culture medium to obtain a concentration of 1 mg/mL. The maximum concentration of dmso in the tests did not exceed 0.1%, at which level no inhibition of amoebal growth occurred.[64,65] ^{1}H NMR spectra of all complexes in [D$_6$]dmso were recorded to test whether the solvent induced any ligand solvolysis, but all were found to be stable at room temperature for several days. Samples were dissolved or suspended by mild sonication in a Sonicleaner bath for a few minutes and then further dilution with medium to a concentration of 0.1 mg/mL. Twofold serial dilutions were made in the wells of a 96-well microtitre plate (Costar) in the medium (170 μL). Each test included metronidazole as the standard amoebicidal drug; control wells (culture medium plus amoebae) were prepared from a confluent culture by pouring off the medium, adding medium (2 mL) and chilling the culture on ice to detach the organisms from the side of the flask. The number of the amoeba per millilitre was estimated with a heamocytometer, and trypan blue exclusion was used to confirm viability. The cell suspension used was diluted to 10^5 organism/mL by adding fresh medium, and 170 μL of this suspension was added to the test and control well in the plate so that the wells were completely filled (total volume, 340 μL). An inoculum of 1.7×10^4 organisms/well was chosen so that confluent, but not excessive, growth took place in control wells. The plate was sealed with expanded polystyrene (0.5 mm), secured with tape, placed in a modular incubating chamber (flow laboratories, High Wycombe, UK) and gassed for 10 min with nitrogen before incubation at 37 °C for 72 h.

Assessment of Antiamoebic Activity: After incubation, the growth of amoebae in the plate was checked with a low-power microscope. The culture medium was removed by inverting the plate and shaking gently. The plate was then immediately washed once in 0.9% NaCl at 37 °C. This procedure was completed quickly, and the plate was not allowed to cool in order to prevent the detachment of amoebae. The plate was allowed to dry at room temperature and the amoebae were fixed with methanol, when dry, and stained with 0.5% aqueous eosin for 15 min. The stained plate was washed once with tap water and then twice with distilled water and allowed to dry. A 200-μL portion of 0.1 N NaOH solutions was added in each well to dissolve the protein and release the dye. The optical density of the resulting solution in each well was determined at 490 nm with a microplate reader. The percentage of inhibition of amoebal growth was calculated from the optical densities of the control and test wells and plotted against the logarithm of the dose of the drug tested. Linear regression analysis was used to determine the best-fit straight line from which the IC_{50} value was found.

MTT Toxicity: The human cervical (HeLa) cells were obtained from NCCS (Pune, India). The cells were cultured in DMEM (Invitrogen) with 10% foetal bovine serum and 1% penicillin/streptomycin. The effect of active compounds **3** and **5**, and the standard drug (metronidazole) on cell proliferation was measured by using an MTT-based assay.[66] Briefly, the cells (6000/well) were incubated in triplicate in a 96-well plate in the presence of various concentrations of compounds **3** and **5** as well as metronidazole or vehicle (dmso) alone in a final volume of 200 μL at 37 °C in a humidified chamber for different time lengths (24, 48 and 72 h). At the end of each time point, 20 μL of MTT solution (5 mg/mL in PBS) was added to each well, and the cells were incubated at 37 °C in a humidified chamber for 4 h. After 4 h, the supernatant was removed from each well. The coloured formazan crystal produced from MTT was dissolved in 200 μL of dmso, and then the absorbance (A) value was measured at 570 nm by a multiscanner autoreader. The following formula was used for the calculation of the percentage of cell viability (CV): CV (%) = (A of the experimental samples/A of the control) × 100.

Preparations

$CH_2(H_2$sal-nah$)_2$ (I) and $CH_2(H_2$sal-inh$)_2$ (II): Ligands $CH_2(H_2$sal-nah$)_2$ (**I**) and $CH_2(H_2$sal-inh$)_2$ (**II**) were prepared according to the literature procedure with slight modifications.[67] A solution of 5,5′-methylenebis(salicylaldehyde) (2.65 g, 10 mmol) was prepared in hot methanol (40 mL) and was added to a solution of appropriate hydrazide (2.743 g, 20 mmol) dissolved in methanol (20 mL) with stirring. The obtained reaction mixture was refluxed on a water bath for 2 h. After reducing the solvent volume to about 30 mL

and cooling to about 10 °C, the solid obtained was filtered, washed with methanol and dried in a desiccator over silica gel.

Data for $CH_2(H_2sal\text{-}nah)_2$ (I): Yield 5.67 g (91%). $C_{27}H_{22}N_6O_4$ (494): calcd. C 65.56, H 4.49, N 17.00; found C 65.36, H 4.41, N 17.22.

Data for $CH_2(H_2sal\text{-}inh)_2$ (II): Yield 5.76 g (92%). $C_{27}H_{22}N_6O_4$ (494): calcd. C 65.56, H 4.49, N 17.00; found C 65.42, H 4.44, N 17.13.

$[CH_2\{V^{IV}O(sal\text{-}nah)(H_2O)\}_2]$ (1): A solution of $CH_2(H_2sal\text{-}nah)_2$ (0.494 g, 1 mmol) was prepared by refluxing in dry methanol (80 mL) and filtered. A filtered solution of $[V^{IV}O(acac)_2]$ (0.530 g, 2 mmol) in dry methanol (15 mL) was added to the above solution while stirring and the reaction mixture was refluxed by means of a water bath for 3 h. After reducing the volume to about 20 mL and keeping at room temperature for 10 h, the separated brown solid was filtered, washed with methanol and dried in a desiccator over silica gel. Yield: 0.451 g (72.3%). μ_{eff}(293 K) = 1.71 μB. $C_{27}H_{22}N_6O_8V_2$ (660.39): calcd. C 49.11, H 3.36, N 12.73; found C 49.0, H 3.41, N 12.52.

$[CH_2\{V^{IV}O(sal\text{-}inh)(H_2O)\}_2]$ (2): Complex **2** was prepared from $[V^{IV}O(acac)_2]$ (0.530 g, 2 mmol) and $CH_2(H_2sal\text{-}inh)_2$ (0.494 g, 1 mmol) according to the method outlined for **1**. Yield: 0.505 g (80.9%). μ_{eff}(293 K) = 1.70 μB. $C_{27}H_{22}N_6O_8V_2$ (660.39): calcd. C 49.11, H 3.36, N 12.73; found C 48.92, H 3.46, N 12.63.

$K_2[CH_2\{V^{V}O_2(sal\text{-}nah)\}_2]\cdot 2H_2O$ (3). Method A: A mixture of $[CH_2\{V^{IV}O(sal\text{-}nah)(H_2O)\}_2]$ (0.312 g, 0.5 mmol) and KOH (0.068 g, 1.2 mmol) in methanol (25 mL) was refluxed for 2 h and then left for aerial oxidation as well as slow evaporation of the solvent at room temperature. Complex **3** slowly precipitated in about 3 d. This was filtered off, washed with cold methanol and dried in a desiccator over silica gel. Yield: 0.265 g (72.0%). **Method B:** A solution of $CH_2(H_2sal\text{-}nah)_2$ (0.494 g, 1 mmol) dissolved in aqueous KOH (0.224 g, 4 mmol) was added with stirring to a filtered aqueous solution of KVO_3 prepared in situ by dissolving vanadium(V) oxide (0.20 g, 2 mmol) in KOH (0.112 g, 2 mmol). The pH of the reaction mixture was adjusted to about 7.5 by adding HCl (4 M). The yellow solid of **3** started to separate and was filtered after 2 h of stirring, washed with water and dried. Yield 0.512 g (69.7%). $C_{27}H_{22}K_2N_6O_{10}V_2$ (770.59): calcd. C 42.08, H 2.88, N 10.91; found C 41.82, H 2.73, N 10.83. ^{51}V NMR [300 MHz, $(CD_3)_2$SO, 25 °C]: δ = –533 ppm.

$Cs_2[CH_2\{V^{V}O_2(sal\text{-}nah)\}_2]\cdot 2H_2O$ (4). Method A: A filtered solution of $[V^{IV}O(acac)_2]$ (0.463 g, 1.75 mmol) in methanol (15 mL) was added while stirring to a solution of $CH_2(H_2sal\text{-}nah)_2$ (0.321 g, 0.65 mmol) prepared as reported for **1** in methanol (80 mL). After adding $CsOH\cdot H_2O$ (0.300 g, 1.78 mmol), the reaction mixture was refluxed for 2 h. The dark red solution obtained was allowed to stand for aerial oxidation and became yellow within 24 h. After reducing the volume to about 10 mL and keeping at room temperature, complex **4** separated within 24 h. This was filtered off, washed with cold methanol and dried in a desiccator over silica gel. Yield 0.653 g (70.8%). $C_{27}H_{22}Cs_2N_6O_{10}V_2$ (958.20): calcd. C 33.84, H 2.31, N 8.77; found C 33.66, H 2.37, N 8.81. ^{51}V NMR [300 MHz, $(CD_3)_2$SO, 25 °C]: δ = –532 ppm. **Method B:** A mixture of $[CH_2\{V^{IV}O(sal\text{-}nah)(H_2O)\}_2]$ (0.312 g, 0.5 mmol) and $CsOH\cdot H_2O$ (0.202 g, 1.2 mmol) in methanol (25 mL) was refluxed for 2 h and then left for aerial oxidation as well as slow evaporation of the solvent at room temperature. Complex **4** slowly precipitated in about 3 d. The rest of the procedure was the same as for method A. Yield 0.39 g (84.6)%.

$Cs_2[CH_2\{V^{V}O_2(sal\text{-}inh)\}_2]\cdot 2H_2O$ (5): This complex was prepared according to the same procedures outlined for $Cs_2[CH_2\{V^{V}O_2(sal\text{-}nah)_2\}]\cdot 2H_2O$. Yield 0.682 g (74.0%). $C_{27}H_{22}Cs_2N_6O_{10}V_2$ (958.20): calcd. C 33.84, H 2.31, N 8.77; found C 33.87, H 2.34, N 8.71. ^{51}V NMR [300 MHz, $(CD_3)_2$SO, 25 °C]: δ = –532 ppm.

Catalytic Reactions

Oxidation of Methyl Phenyl Sulfide and Diphenyl Sulfide: Methyl phenyl sulfide (1.24 g, 10 mmol) or diphenyl sulfide (1.86 g, 10 mmol) and aqueous 30% H_2O_2 (2.27 g, 20 mmol) were added to petroleum ether (10 mL). After addition of catalyst precursors [oxidovanadium(IV) complexes **1** or **2**, 0.020 g] to the above mixture, the reaction mixture was stirred at room temperature for 7 h. During this period, the products formed were analysed by gas chromatography withdrawing small aliquots at fixed time intervals and the identity of the products confirmed using GC–MS.

Oxidative Bromination of Salicylaldehyde: Complexes $K_2[CH_2\{V^{V}O_2(sal\text{-}nah)\}_2]\cdot 2H_2O$, $Cs_2[CH_2\{V^{V}O_2(sal\text{-}nah)\}_2]\cdot 2H_2O$ and $Cs_2[CH_2\{V^{V}O_2(sal\text{-}inh)\}_2]\cdot 2H_2O$ were used as catalysts to carry out oxidative bromination. In a typical reaction, salicylaldehyde (2.44 g, 20 mmol) was added to an aqueous solution (40 mL) of KBr (5.95 g, 50 mmol), followed by addition of aqueous 30% H_2O_2 (13.62 g, 120 mmol) in a 100-mL reaction flask. The catalyst (0.02 g for **4** and **5**, and 0.016 g for **3**) and 70% $HClO_4$ (2.86 g, 20 mmol) were added, and the reaction mixture was stirred at room temperature. Three additional 20-mmol portions of 70% $HClO_4$ were further added to the reaction mixture in three equal portions at half-hour intervals under continuous stirring. After 7 h, the white product that had separated was filtered off, washed with water and dried. The crude mass was dissolved in CH_2Cl_2; insoluble material, if any, was removed by filtration, and the solvent evaporated. A CH_2Cl_2 solution of this material was subjected to gas chromatography and the identity of the products confirmed by GC–MS.

Supporting Information (see footnote on the first page of this article): IR, ^{1}H and ^{13}C NMR spectra of complexes, details of solution studies of complexes **3** and **4**, figures dealing with the details of the optimisation of the reactions conditions for the catalytic reactions.

Acknowledgments

M. R. M. and A. A. K. are thankful to the Council of Scientific and Industrial Research for financial support. J. C. P. and A. K. thank the Portuguese NMR Network (IST-UTL Center) and the POCI 2010, FEDER, Fundação para a Ciência e Tecnologia (SFRH/BPD/34835/2007) for financial support.

[1] S. Raugei, P. Carloni, *J. Phys. Chem. B* **2006**, *110*, 3747–3758.
[2] G. Santoni, G. Licini, D. Rehder, *Chem. Eur. J.* **2003**, *9*, 4700–4708.
[3] V. M. Dembitsky, *Tetrahedron* **2003**, *59*, 4701–4720.
[4] G. Zampella, P. Fantucci, V. L. Pecoraro, L. De Gioia, *J. Am. Chem. Soc.* **2005**, *127*, 953–960.
[5] D. G. Fujimori, C. T. Walsh, *Curr. Opin. Chem. Biol.* **2007**, *11*, 553–560.
[6] C. Drago, L. Caggiano, R. F. W. Jackson, *Angew. Chem. Int. Ed.* **2005**, *44*, 7221–7223.
[7] M. E. Cucciolito, R. Del Litto, G. Roviello, F. Ruffo, *J. Mol. Catal. A* **2005**, *236*, 176–181.
[8] A. L. Maciuca, C. E. Ciocan, E. Dumitriu, F. Fajula, V. Hulea, *Catal. Today* **2008**, *138*, 33–37.
[9] I. Lippold, J. Becher, D. Klemmb, W. Plass, *J. Mol. Catal. A* **2009**, *299*, 12–17.
[10] C. Wikete, P. Wu, G. Zampella, L. De Gioia, G. Licini, D. Rehder, *Inorg. Chem.* **2007**, *46*, 196–207.
[11] K. H. Thompson, C. Orvig, *J. Inorg. Biochem.* **2006**, *100*, 1925–1935.

[12] K. H. Thompson, J. Lichter, C. LeBel, M. C. Scaife, J. H. McNeill, C. Orvig, *J. Inorg. Biochem.* **2009**, *103*, 554–558.
[13] M. Tanyuksel, W. A. Petri Jr, *Clin. Microbiol. Rev.* **2003**, *16*, 713–729.
[14] S. L. Stanley Jr, *Lancet* **2003**, *361*, 1025–1034.
[15] D. W. Kim, J. M. Park, B. W. Yoon, M. J. Baek, J. E. Kim, S. Kim, *J. Neurol. Sci.* **2004**, *224*, 107–111.
[16] A. F. el-Nahas, I. M. el-Ashmawy, *Basic Clin. Pharmacol. Toxicol.* **2004**, *94*, 226–231.
[17] V. Purohit, A. K. Basu, *Chem. Res. Toxicol.* **2000**, *13*, 673–692.
[18] P. Abboud, V. Lemee, G. Gargala, P. Brasseur, J. J. Ballet, F. Borsa-Lebas, F. Caron, L. Favennec, *Clin. Infect. Dis.* **2001**, *32*, 1792–1794.
[19] W. Petri, *Trends Parasitol.* **2003**, *19*, 523–526.
[20] Shailendra, N. Bharti, M. T. Gonzalez Garza, D. E. Cruz-Vega, J. C. Garza, K. Saleem, F. Naqvi, A. Azam, *Bioorg. Med. Chem. Lett.* **2001**, *11*, 2675–2678.
[21] Y. Q. Zuo, W. P. Liu, Y. F. Niu, C. F. Tian, M. J. Xie, X. Z. Chen, L. Li, *J. Pharm. Pharmacol.* **2008**, *60*, 1335–1340.
[22] D. A. Roess, S. M. Smith, P. Winter, J. Zhou, P. Dou, B. Baruah, A. M. Trujillo, N. E. Levinger, X. Yang, B. G. Barisas, D. C. Crans, *Chem. Biodivers.* **2008**, *5*, 1558–1570
[23] A. Anwar-Mohamed, A. O. El-Kadi, *Drug Metab. Dispos.* **2008**, *36*, 1819–1827.
[24] A. M. Evangelou, *Crit. Rev. Oncol. Hematol.* **2002**, *24*, 249–265.
[25] M. R. Maurya, S. Agarwal, M. Abid, A. Azam, C. Bader, M. Edel, D. Rehder, *Dalton Trans.* **2006**, 937–947.
[26] M. R. Maurya, A. Kumar, A. R. Bhat, A. Azam, C. Bader, D. Rehder, *Inorg. Chem.* **2006**, *45*, 1260–1269.
[27] S. P. Perlepes, D. Nicholls, M. R. Harison, *Inorg. Chim. Acta* **1985**, *102*, 137–143.
[28] M. R. Maurya, S. Khurana, Shailendra, A. Azam, W. Zhang, D. Rehder, *Eur. J. Inorg. Chem.* **2003**, 1966–1973.
[29] M. R. Maurya, S. Agarwal, C. Bader, D. Rehder, *Eur. J. Inorg. Chem.* **2005**, 147–157.
[30] O. Bortolini, M. Carraro, V. Conte, S. Moro, *Eur. J. Inorg. Chem.* **1999**, 1489–1495.
[31] O. Bortolini, V. Conte, F. Di Furia, S. Moro, *Eur. J. Inorg. Chem.* **1998**, 1193–1197.
[32] C. Slebodnick, V. L. Pecoraro, *Inorg. Chim. Acta* **1998**, *283*, 37–43.
[33] P. Schwendt, K. Liscak, *Collect. Czech. Chem. Commun.* **1996**, *61*, 868–876.
[34] M. J. Clague, N. L. Keder, A. Butler, *Inorg. Chem.* **1993**, *32*, 4754–4761.
[35] M. R. Maurya, A. Arya, A. Kumar, J. Costa Pessoa, *Dalton Trans.* **2009**, 2185–2195.
[36] M. Casný, D. Rehder, *Dalton Trans.* **2004**, 839–846.
[37] J. S. Jaswal, A. S. Tracey, *Inorg. Chem.* **1991**, *30*, 3718–3722.
[38] Q. Zeng, H. Wang, T. Wang, Y. Cai, W. Weng, Y. Zhao, *Adv. Synth. Catal.* **2005**, *347*, 1933–1936.
[39] M. R. Maurya, S. Agarwal, C. Bader, M. Ebel, D. Rehder, *Dalton Trans.* **2005**, 537–544.
[40] J. A. Bonadies, W. M. Butler, V. L. Pecoraro, C. J. Carrano, *Inorg. Chem.* **1987**, *26*, 1218–1222.
[41] J. A. Bonadies, C. J. Carrano, *J. Am. Chem. Soc.* **1986**, *108*, 4088–4095.
[42] W. Plass, A. Pohlmann, H.-P. Yozgatli, *J. Inorg. Biochem.* **2000**, *80*, 181–183.
[43] K. Fukui, H. Ohya-Nishiguchi, H. Kamada, *Inorg. Chem.* **1998**, *37*, 2326–2327.
[44] A. Rockenbauer, L. Korecz, *Appl. Magn. Reson.* **1996**, *10*, 29–43.
[45] K. Wurthrich, *Helv. Chim. Acta* **1965**, *48*, 1012–1017.
[46] N. D. Chasteen in *Biological Magnetic Resonance* (Ed.: J. Reuben), Plenum, New York, **1981**, p. 53.
[47] D. Rehder, *Bioinorganic Vanadium Chemistry*, Wiley & Sons, New York, **2008**.
[48] I. Correia, J. Costa Pessoa, M. T. Duarte, R. T. Henriques, M. F. M. Piedade, L. F. Veiros, T. Jackush, A. Dornyei, T. Kiss, M. M. C. A. Castro, C. F. G. C. Geraldes, F. Avecilla, *Chem. Eur. J.* **2004**, *10*, 2301–2317.
[49] A. G. J. Ligtenbarg, R. Hage, B. L. Feringa, *Coord. Chem. Rev.* **2003**, *237*, 89–101.
[50] B. J. Hamstra, G. J. Colpas, V. L. Pecoraro, *Inorg. Chem.* **1998**, *37*, 949–955.
[51] A. Giacomelli, C. Floriani, A. O. S. Duarte, A. Chiesi-Villa, C. Guastini, *Inorg. Chem.* **1982**, *21*, 3310–3316.
[52] M. A. Anderson, A. Willets, S. Allenmark, *J. Org. Chem.* **1997**, *62*, 8455–8458.
[53] H. B. ten Brink, H. E. Schoemaker, R. Wever, *Eur. J. Biochem.* **2001**, *268*, 132–138.
[54] G. J. Colpas, B. J. Hamstra, J. W. Kampf, V. L. Pecoraro, *J. Am. Chem. Soc.* **1996**, *118*, 3469–3478.
[55] A. Butler, M. J. Clague, G. E. Meister, *Chem. Rev.* **1994**, *94*, 625–638.
[56] C. J. Schneider, J. E. Penner-Hahn, V. L. Pecoraro, *J. Am. Chem. Soc.* **2008**, *130*, 2712–2713.
[57] P. Adão, J. Costa Pessoa, R. T. Henriques, M. L. Kuznetsov, F. Avecilla, M. R. Maurya, U. Kumar, I. Correia, *Inorg. Chem.* **2009**, *48*, 3542–3561.
[58] A. M. Ramadan, *J. Inorg. Biochem.* **1997**, *65*, 183–189.
[59] B. J. Winer, *Statistical Principals in Experimental Design*, 2nd ed., McGraw-Hill, New York, **1971**, vol. 22, p. 45.
[60] R. A. Rowe, M. M. Jones, *Inorg. Synth.* **1957**, *5*, 113.
[61] R. L. Dutta, A. Syamal, *Elements of Magnetochemistry*, 2nd ed., Affiliated East-West Press, New Delhi, **1993**, p. 8.
[62] C. W. Wright, M. J. O'Neill, J. D. Phillipson, D. C. Warhurst, *Antimicrob. Agents Chemother.* **1988**, *32*, 1725–1729.
[63] L. S. Diamond, D. R. Harlow, C. C. Cunnick, *Trans. R. Soc. Trop. Med. Hyg.* **1978**, *72*, 431–432.
[64] F. D. Gillin, D. S. Reiner, M. Suffnes, *Antimicrob. Agents Chemother.* **1982**, *22*, 342–345.
[65] A. T. Keen, A. Harris, J. D. Phillipson, D. C. Warhurst, *Planta Med.* **1986**, 278–284.
[66] T. Mosmann, *J. Immunol. Methods* **1983**, *65*, 55–63.
[67] M. R. Maurya, D. C. Antony, S. Gopinathan, C. Gopinathan, *Indian J. Chem. Sect. A* **1995**, *34*, 967–970.

Received: July 20, 2009
Published Online: October 29, 2009

